Crossover from Poisson to Wigner-Dyson level statistics in spin chains with integrability breaking

D. A. Rabson

Department of Physics, University of South Florida, Tampa, Florida 33620, USA

B. N. Narozhny

Condensed Matter Section, ICTP, Strada Costiera 11, I-34100, Trieste, Italy

A. J. Millis

Physics Department, Columbia University, 538 West 120th Street, New York, New York 10027, USA

We study numerically the evolution of energy-level statistics as an integrability-breaking term is added to the XXZ Hamiltonian. For finite-length chains, physical properties exhibit a crossover from behavior corresponding to the Poisson level statistics characteristic of integrable models to behavior corresponding to the Wigner-Dyson statistics characteristic of the random-matrix theory used to describe chaotic systems. Different measures of the level statistics are observed to follow different crossover patterns. The range of numerically accessible system sizes is too small to establish with certainty the scaling with system size, but the evidence suggests that in a thermodynamically large system an infinitesimal integrability breaking would lead to Wigner-Dyson behavior.

I. INTRODUCTION

The conjecture that the statistical properties of energy levels of chaotic quantum systems may be described in terms of the theory of random matrices is widely accepted in various fields of physics.[1] This however is not a universal property of all complex interacting systems. One example to the contrary is provided by the class of the so-called integrable models,[2] where the behavior of the system is completely described by a large (infinite in the thermodynamic limit) set of conserved quantities. One consequence is that the level-spacing distribution $P_\Delta(E)$ in the case of integrable models is the Poisson distribution (Δ denotes mean level spacing),

$$P_\Delta(E) = \frac{1}{\Delta} e^{-E/\Delta}, \tag{1}$$

whereas in random-matrix theory the distribution takes the Wigner-Dyson form,

$$P_\Delta(E) = b_\beta \left(\frac{E}{\Delta}\right)^\beta e^{-a_\beta E^2/\Delta^2}, \tag{2}$$

where $\beta = 1$, 2, 4 correspond to orthogonal, unitary, and symplectic ensembles respectively, and[3] $b_1 = \pi/2$, $a_1 = \pi/4$; $b_2 = 32/\pi^2 \approx 3.24$, $a_2 = 4/\pi$; $b_4 = 262144/729\pi^3 \approx 11.6$, $a_4 = 64/9\pi \approx 2.26$.

Other statistical properties (for example, the evolution of levels under an external perturbation[4]) also differ for the two cases. One important class of external perturbations is the application of a voltage. The difference in response in this case leads to spectacular differences in transport properties of integrable and nonintegrable models. Integrable models have been argued to have an infinite conductivity even at high temperatures, essentially because a typical level has a large response to a voltage, whereas nonintegrable models have a finite conductivity because a typical level has a small response.[5,6]

While these basic properties have been established for the two generic cases of integrable and nonintegrable models, the crossover between these two limits as an integrability-breaking interaction is turned on has not been carefully studied to our knowledge, nor have the implications of the crossover for the finite-size conductivity of nearly integrable systems been determined. Two of us, with N. Andrei, presented a few numerical results in a paper mainly concerned with the charge transport of integrable systems.[7] However, the significance and interpretation of these results were not clear. Song and Shepelyansky[8] studied the effects of a random potential on level statistics of two-dimensional (2D) interacting Fermions and found evidence for a localization-delocalization transition. However, in their case, the physics of the transition is due to the disorder and thus is different from the situation in integrable models. Berkovits and Avishai also study the crossover in the presence of disorder.[9] Earlier work by DiStasio and Zotos[10] noted a crossover between Poisson and Wigner-Dyson in the low-energy part of the spectrum and did not address scaling with system size. Most recently, Kudo and Deguchi[11] have characterized the probability distribution in the crossover regime as an average between Poisson and Wigner-Dyson, but their numbers were limited to 16 sites, and they do not report the scaling we describe here.

In this paper we will fill these gaps by providing numerical results for finite-size chains with Hamiltonian given by the (integrable) XXZ model plus an integrability-breaking perturbation δH. Our principal results are computations, for finite-length chains, of the crossover from behavior characteristic of Poisson to behavior characteristic of Wigner-Dyson statistics in various statistical measures. These crossovers fail to display an obvious universality in the sense that

different measures show different behavior depending on the XXZ asymmetry parameter and system size.

Our computations are performed for finite-size systems. An important issue is the behavior in the limit of a thermodynamically large system. Extrapolation to the thermodynamic limit proves to be ambiguous for most of the measures we employ (namely, we cannot rule out a saturation of the crossover scales as functions of the system size for chains much longer than those considered in this study), but the data suggest that all the crossover scales vanish at infinite system size.

The rest of the paper is organized as follows. First we discuss the model used in numerical calculations and, in particular, define numerically the value of the integrability-breaking parameter at which a gap appears in the spectrum. All further considerations will be devoted to the gapless regime. Then we discuss the level-spacing distribution and the correlator of level velocities. The latter is related to the parametric statistics of the system and also to its transport properties. For disordered systems, the correlator of level velocities was shown to correspond to the dimensionless conductance of the system, while if one restricts the analysis to periodic boundary conditions only (see below) it coincides with the Drude weight. Discussion of the Drude weight concludes the paper.

II. THE MODEL

We study the effect of integrability breaking on the physical properties of a spin chain. The integrable model we consider is the XXZ chain defined on a N-site ring with periodic boundary conditions in the presence of external flux ϕ threading the ring:

$$H_{XXZ} = \frac{1}{2} \sum_{i=1}^{N} (e^{i\varphi/N} S_i^+ S_{i+1}^- + e^{-i\varphi/N} S_i^- S_{i+1}^+)$$
$$+ \sum_{i=1}^{N} J_1 S_i^z S_{i+1}^z. \qquad (3)$$

(Alternatively, the flux can be gauged out to the boundary, resulting in twisted boundary conditions.) As is well-known, statistical properties of integrable models are governed by the Poisson distribution, Eq. (1). Transport properties of the model can also be inferred from studying the energy levels of the model, namely, by their response to the flux ϕ. At zero temperature the behavior of the ground-state energy of the system under slow variation of the flux determines the Drude weight or the stiffness[12] $\mathcal{D}_s$ as

$$\mathcal{D}_s = \frac{N}{2} \frac{\partial^2 E_0}{\partial \phi^2}\bigg|_{\phi \to 0}.$$

Nonvanishing $\mathcal{D}_s$ signals ballistic transport in the system. For the XXZ model at $T=0$ this is the case[13] for $-1 < J_1 < 1$, where excitations of the system are gapless. If $|J_1| > 1$, then the excitation spectrum of the model is gapped,[14] and $\mathcal{D}_s = 0$. At finite temperatures the above expression for the stiffness can be generalized[5–7] to $\mathcal{D}_s = D_1 + D_2$, where

$$D_1 = -\frac{N}{2\beta} \frac{1}{\mathcal{Z}} \frac{\partial^2 \mathcal{Z}}{\partial \phi^2}\bigg|_{\phi \to 0}$$

vanishes in the thermodynamic limit,[15] and the remaining term, D_2, is *positive*:

$$D_2 = \frac{\beta N}{2} \frac{1}{\mathcal{Z}} \sum_n \left(\frac{\partial E_n}{\partial \phi}\right)^2 \bigg|_{\phi \to 0} e^{-\beta E_n}. \qquad (4)$$

In the gapless phase of the XXZ model it has been shown[5–7] that ballistic transport persists to finite temperatures in the sense that $D(N) = \lim_{T \to \infty} D_2(N) T > 0$. The infinite-temperature limit of this result implies that for a typical level $dE_n/d\phi \sim 1/\sqrt{N}$. At the antiferromagnetic Heisenberg point $J_1 = 1$ the model still has gapless excitations, but results of Fabricius and McCoy[16] suggest that D_2 vanishes (slowly) as the system size increases. Numerical results of Narozhny *et al.*[7] were consistent with this suggestion, but the limited range of system sizes attainable precluded a definite statement.

Integrability breaking is introduced by adding the term with next-neighbor coupling

$$\delta H = \sum_{i=1}^{N} J_2 S_i^z S_{i+2}^z. \qquad (5)$$

This term should be contrasted to that considered by Eggert[17] insofar as it is explicitly not SU(2) invariant. However, away from the Heisenberg point the effect of the interaction Eq. (5) is similar to that of its SU(2)-invariant counterpart: (i) it breaks the integrability of the system and (ii) for large enough values of J_2 it causes the system to dimerize, so that the spectrum acquires a gap. The critical value of J_2 at which the gap opens is of course different from the 0.24 found in Ref. 17. Our numerical estimates[18] suggest a value $J_2^{(c)} \gtrsim 1.1$ that is a weakly increasing function of both system size and J_1: for $N = 18$ and $J_1 = 0.2$, for example, the gap appears to open at $J_2 = 1.13 \pm 0.01$. The gap opening limits the range of values of J_2 under consideration, as we are interested only in properties of the gapless phase; indeed, the measures we consider presently begin showing different behavior for $J_2 > J_2^{(c)}$. Similarly, the parameter region considered by Faas *et al.*[4] belongs to the gapped regime, which accounts for certain differences in the behavior of the level statistics reported in Ref. 4 and in the present paper.

In this paper we study the eigenvalues of $H = H_{XXZ} + \delta H$ and their evolution under change of ϕ for the above model with varying $J_{1,2}$ and system size. For the nonintegrable Hamiltonian $H_{XXZ} + \delta H$ we use exact numerical diagonalization to construct the level-spacing distribution and level auto-correlation functions and to evaluate the stiffness D_2, Eq. (4). The use of exact numerical methods is motivated by the need to obtain the whole spectrum of the model in order (i) to study the statistical properties of the spectrum and (ii) to study the stiffness Eq. (4) at infinite temperature. The drawback of the method is the limitation to
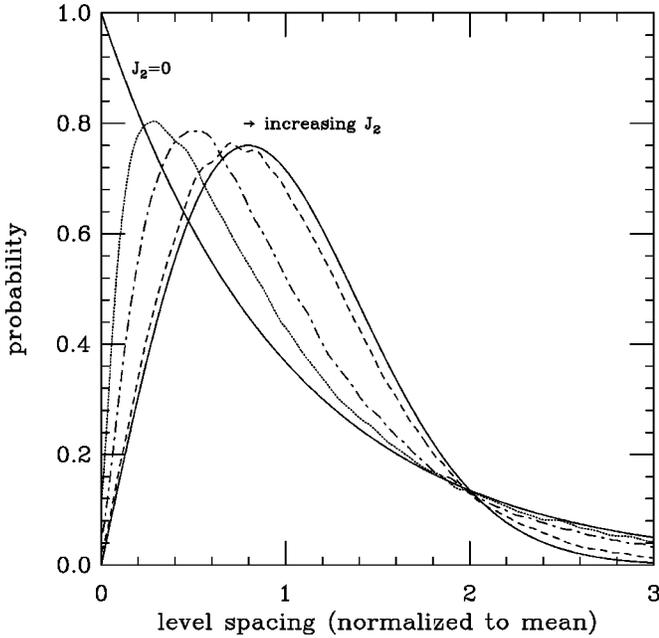
FIG. 1. Typical crossover of the level-spacing distribution from Poisson (left solid curve) for $J_2=0$ to Wigner-Dyson (right solid curve) for a representative system. The plot is made for $N=18$, $S^z=3$, $J_1=0.2$, momentum $k=0$, and $J_2=0.1,0.2,0.5$. For $J_2=0$ the numerical distribution agrees very closely with the exponential plotted. The Wigner-Dyson distribution shown is the theoretical curve for the orthogonal ensemble.

small system sizes (we present results for chains of up to 20 sites). For finite system sizes we obtain a detailed characterization of the crossover.

III. LEVEL-SPACING DISTRIBUTION

We begin with a brief discussion of the integrable case. The level-spacing distribution for $J_2=0$ is the Poisson distribution (shown in Fig. 1 by the left solid curve). This illustrates the fact that the integrable system has so many conservation laws that levels essentially do not repel each other. To characterize transport properties of the system we show in Fig. 2 the quantity $D(N)=D_2(N)T$ at $T\rightarrow\infty$ for different system sizes and different values of the integrable interaction J_1 (dashed lines in Fig. 2). D is seen to be almost size independent for the cases $J_1<1$, in agreement with previous work,[7] while a weak size dependence is evident in the Heisenberg case $J_1=1$. Although this dependence appears to have a positive y intercept, we believe that the system size in this study is still too small to make a definite statement regarding the behavior of the Heisenberg model in the thermodynamic limit.[19]

We turn now to the case of broken integrability. As the integrability-breaking term Eq. (5) is added to the Hamiltonian, energy levels immediately start to repel,[20] and as a consequence immediately $P_\Delta(0)=0$ so that the distribution acquires a peak. As illustrated in Fig. 1, increasing J_2 shifts the peak to the right until the distribution starts to look like the Wigner-Dyson distribution (shown in Fig. 1 by the right solid curve). At the same time the tail of the distribution
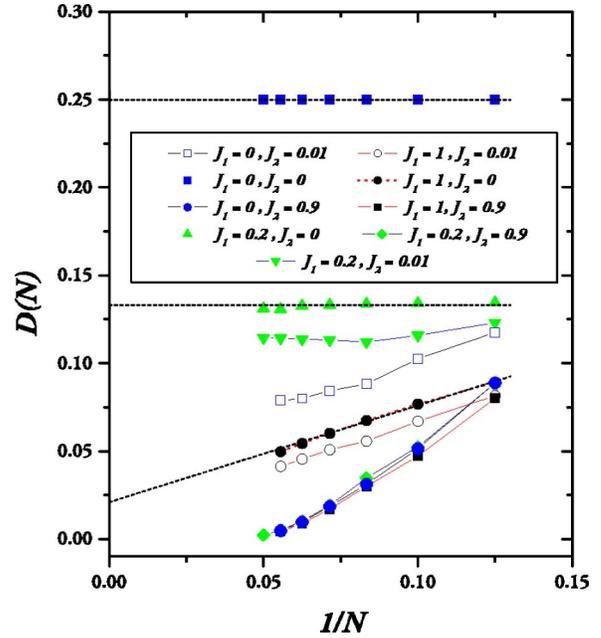

FIG. 2. (Color online) The stiffness $D(N)=\lim_{T\rightarrow\infty}D_2(N)T$ as a function of inverse system size for different values of interaction parameters. Dashed lines show a naive extrapolation to the thermodynamic limit for the integrable system. Here we show the results for $J_1=0$ (squares), $J_1=0.2$ (triangles) and $J_1=1$ (circles). Empty symbols correspond to the smallest $J_2=0.01$, which seems to affect strongly only the $J_1=0$ case. The behavior for $J_2=0.9$ appears to be independent of J_1.

changes from the exponential in Eq. (1) to the (asymptotically) Gaussian tail of the Wigner-Dyson distribution.

To quantify this crossover we show the evolution of the peak position and the characteristics of the tail with the change in J_2 in Figs. 3 and 4. Both exhibit similar features, although the estimates for the crossover scales extracted from the two are numerically different (see Table I and insets in Figs. 3 and 5).

As shown in Fig. 3, the peak of the distribution grows from zero to the value characteristic of the Wigner-Dyson distribution and then saturates. To estimate the crossover scale J_2^*, we fit the data by the hyperbolic tangent[21] of the form $a\tanh(x/x_0)$ with x_0 approximating J_2^*. The inset shows the resulting values for J_2^* as a function of the system size. As we noted before,[20] we are restricting our attention to fixed values of the total spin S^z. However, for the purposes of the finite-size scaling, it makes more sense to compare data with the fixed ratio S^z/N. One way to see this is to recall that by means of the Jordan-Wigner transformation the spin chain can be mapped onto a system of spinless Fermions.[7] In the Fermion language, $1/2-S^z/N$ corresponds to the filling fraction. Since it is not possible to keep the ratio S^z/N exactly the same for all values of N used in this paper, we choose to present the data for two sectors of fixed S^z that are closest to the chosen value of S^z/N. Therefore the inset in Fig. 3 shows two data points for the N other than $N=18$ (we chose $S^z/N=1/6$). The straight lines are just guides to the eye.

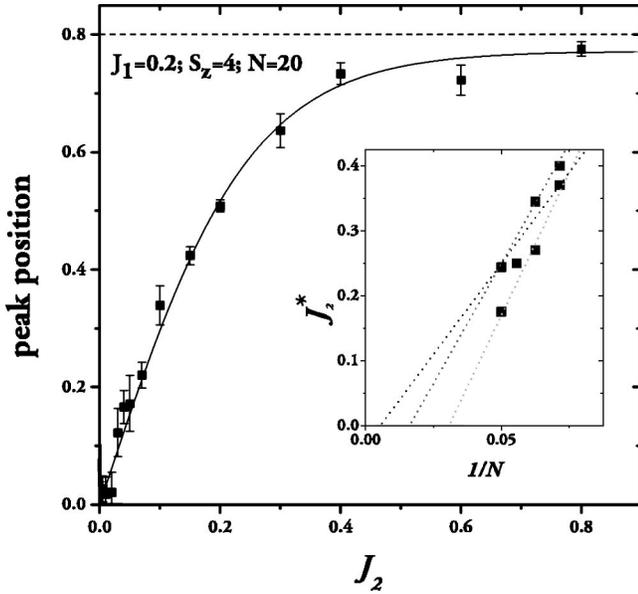To analyze the evolution of the tail, we approximate the

FIG. 3. Typical crossover of the peak position. The data correspond to $N=20$, $S^z=4$, $J_1=0.2$, momentum $k=0$, with the solid line a fit to the form $a \tanh(J_2/J_2^*)$, $J_2^* \approx 0.25$. The dashed line indicates the peak position of the Wigner-Dyson distribution. The inset shows finite-size scaling of the crossover scale (the data points correspond to $N=20$, $S^z=4$; $N=20$, $S^z=3$; $N=18$, $S^z=3$; $N=16$, $S^z=3$; $N=16$, $S^z=2$; $N=14$, $S^z=3$; $N=14$, $S^z=2$); the straight lines are guides to the eye, suggesting that J_2^* vanishes for the infinite chain.
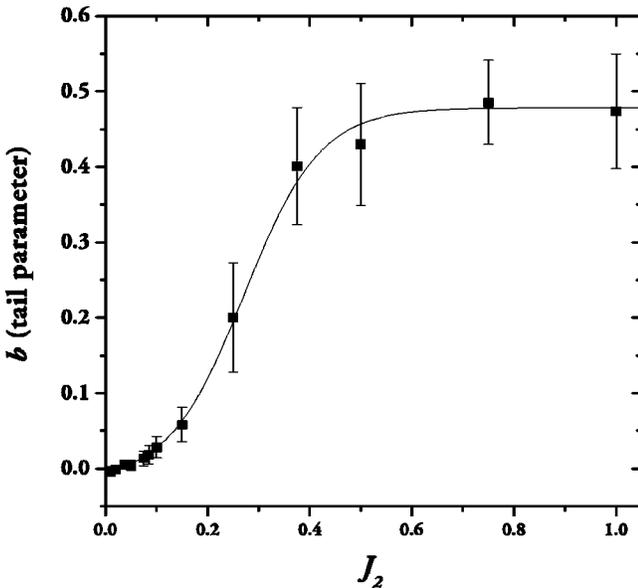
TABLE I. The system crosses over from integrable to fully chaotic behavior with *different* crossover scales, depending on what is being measured. Furthermore, the crossover scales themselves scale differently with system size. We calculate crossover scales associated with peak position, tail crossover (from exponential to Gaussian), mean squared level velocity C_0, the fourth cumulant k_4 of the level-spacing distribution, and conductance D_2T. In this example, $J_1=0.2$. The crossover $J_2^{*D_2T}$ is calculated for the entire spectrum, while all the others are calculated for the $S^z=3$ sector and momentum $k=0$. Entries of $-$ could not be extracted from the data because of numerical uncertainty. Rough error estimates for the least significant digit are provided where available.

N	$J_2^{*\mathrm{peak}}$	$J_2^{*\mathrm{tail}}$	$J_2^{*C_0}$	$J_2^{*k_4}$	$J_2^{*D_2T}$
20	0.19	0.27	0.097(4)	0.091	0.079(3)
18	0.25	0.43	0.15(1)	0.17	0.107(3)
16	0.34	0.49	0.20(2)	0.24	0.145(2)
14	0.38	$-$	0.28(2)	$-$	0.178(5)

intermediate distributions (see Fig. 1) by

$$P_\Delta(E) \propto \exp\left[-a\frac{E}{\Delta} - b\left(\frac{E}{\Delta}\right)^2 \right].$$

Clearly, for Eq. (1) $a=1$ and $b=0$, while for the orthogonal ensemble, Eq. (2) corresponds to $a=0$ and $b=\pi/4$. In Fig. 4 we show the evolution of b (the fact that plotted values never reach $\pi/4$ is an artifact of the calculation). Fitting the curve to a hyperbolic tangent, we can extract an estimate for the crossover value $J_2^*(N=20)=0.27$. This value differs somewhat from the one extracted from the peak position (for the
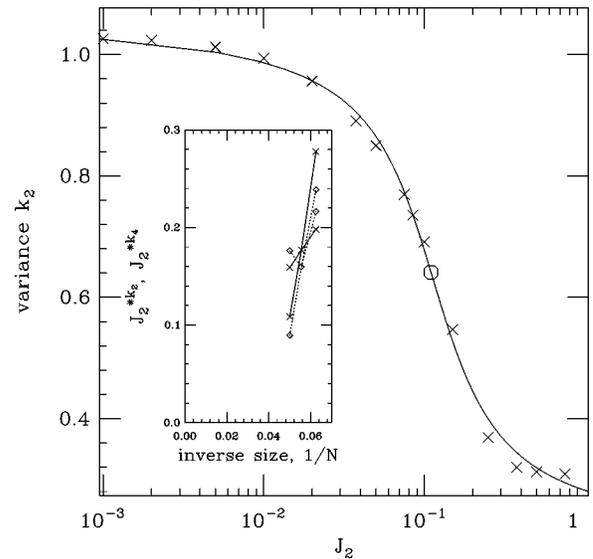

FIG. 4. Evolution of the parameter b from the tail of the level-spacing distribution. For the integrable case, $b=0$. For large J_2 it does not quite reach the Wigner-Dyson value $\pi/4$, but it still shows a clear crossover. The crossover scale estimated by fitting the data to a hyperbolic tangent is $J_2^*=0.27$. The plot is made for $N=20$, $S^z=3$, $J_1=0.2$, and momentum $k=0$.

FIG. 5. Variance estimate ($\times$), k_2, as a function of J_2 for system size $N=20$. ($J_1=0.2$, $S^z=3$, momentum $k=0$.) The crossover scale is estimated as the turning point ($\bigcirc$) in a tanh fit (curve). The inset illustrates the finite-size scaling for cumulants k_2 (solid lines and $\times$) and k_4 (dotted lines and $\diamond$) for the same set of sizes and S^z sectors as in Figs. 3 and 7 appropriate for 1/3 filling. The J_2^* associated with either cumulant may vanish in the limit of infinite size.

same values of N, S^z, and J_1); see the inset in Fig. 3. The behavior of the tail characteristics with respect to changing system size exhibits the same trend as shown in the inset in Fig. 3 for the peak position: the characteristic scales tend to decay with increasing system size. The naive extrapolation of such a trend is consistent with a statement of vanishing J_2^* as $N \to \infty$; however, the data are insufficient to prove it.

Another way to quantify the evolution of the level-spacing distribution shown in Fig. 1 is to consider cumulants.[22] Their unbiased estimators (the Fisher statistics[23] k_n) are easily computed. For our normalized level spacings, the first cumulant (which is equal to the mean) is unity.

The cumulants of a distribution characterize its width (second cumulant, or variance) and shape;[24] beyond perhaps the fifth, numerical cumulants become too sensitive to outliers to be of much use. A study of the cumulants of a distribution is qualitatively similar to our foregoing study of the tails, but it turns out to be simpler numerically. In Fig. 5 we show the unbiased variance estimate, k_2, as a function of J_2 for system size $N=20$, $J_1=0.2$, $S^z=3$, momentum $k=0$. The theoretical limits should be 1 for the Poisson distribution and $\pi/4 - 1 = 0.2732$ (the bottom of the scale) for Wigner-Dyson. The fact that the data points deviate from these ideal values is an artifact of finite sampling. Fitting the curve to a hyperbolic tangent, we estimate the crossover scale, shown in the inset as a function of size (for the same sequence of quantum numbers as in Fig. 3). The inset also shows the crossover scale for the fourth cumulant. As before, the scaling suggests (but does not establish) that the crossover scale J_2^* associated with either cumulant should vanish in the limit of infinite size. It is not possible to determine whether the different measures, k_2 and k_4 (we also looked at k_3), scale in the same way or differently with system size.

The second cumulant k_2 plays a role similar to that of the parameter η used in Ref. 8 to estimate the overall "proximity" of the observed distribution to either the Poisson or the Wigner-Dyson limit. In that sense, Fig. 5 shows behavior similar to that found in Ref. 8, although the physics of the evolution of levels is quite different in our case.

IV. ELEMENTS OF THE PARAMETRIC STATISTICS

More information about the crossover to the chaotic behavior described by the Wigner-Dyson statistics can be extracted from the study of the autocorrelation functions. Here we will discuss the autocorrelation of level velocities

$$C(\phi) = \frac{1}{\Delta^2} \left\langle \frac{\partial E_i(\theta)}{\partial \theta} \frac{\partial E_i(\theta+\phi)}{\partial \theta} \right\rangle_{\theta, i}, \qquad (6)$$

where the angular brackets indicate averaging over a set of levels and fluxes.[4]

A typical form of the autocorrelation function Eq. (6) is shown in Fig. 6. For large values of J_2, this form resembles the universal correlator characteristic of chaotic systems.[4] However, in the crossover region, $C(\phi)$ deviates from the universal form in a rather complex fashion, which makes a quantitative analysis of the crossover difficult. Therefore we focus on two particular features of the curve, the turning
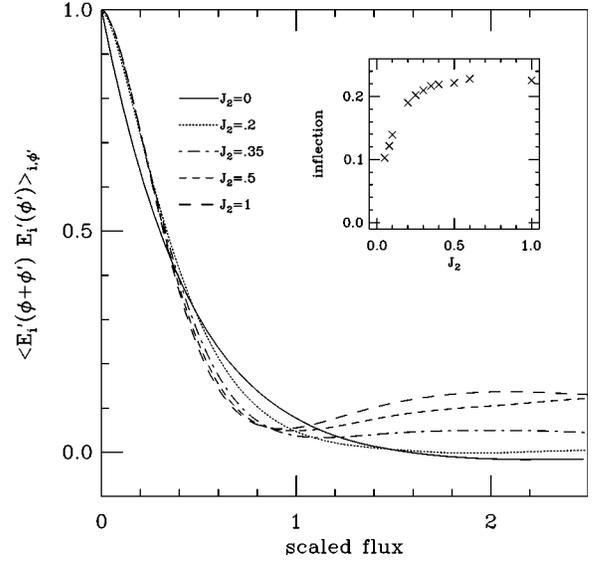

FIG. 6. Autocorrelation of level velocities for various values of integrability breaking. Only a short range of flux is shown; in all cases, the sum rule [the integral of $C(\phi)$ over all fluxes vanishing] is satisfied numerically. For $J_2 > 0$, there is a point of inflection at nonzero flux. However, the integrable model has no initial inflection. The inset plots the position of the inflection point as a function of J_2. These data were derived for $N=20$, $S^z=3$, $J_1=0.2$, $k=0$.

point and $C(0)$. We note a feature of the autocorrelation curve shown in Fig. 6 that appears only as the integrability breaking is introduced: all curves for $J_2 > 0$ have a nonzero point of inflection as the autocorrelation decreases with the increase of J_2, but the autocorrelation function of the integrable system does not have such an inflection point. Consequently, the behavior near zero flux changes from linear $[C(\phi) - C(0) \propto -\phi]$ for the integrable case to quadratic for $J_2 > 0$.

The autocorrelation function of level velocities at zero flux difference $C(0)$ is somewhat similar to the stiffness Eq. (4), the differences being that $C(0)$ is also averaged over a set of fluxes, does not contain the extra factors of temperature and system size, and corresponds to a single sector of fixed S^z. However, in chaotic systems it is $C(0)$ that can be related to transport.[4] There it was argued to correspond to the dimensionless conductance.

In Fig. 7 we show the behavior of $C(0)$ as a function of J_2. Clearly, for finite systems, $C(0)$ exhibits a well-defined crossover. For the dataset presented in Fig. 7 ($N=20$, $J_1 = 0.2$, $S^z = 3$), the correlator $C(0)$ decays as a $\approx 5/2$-power law after J_2 exceeds the value $J_2^{*C_0} = 0.097 \pm 0.004$ (defined in Fig. 7 as a crossing point of the above power law—the straight line in the log-log scale—with the value at $J_2 = 0$).

The inset shows the crossover scale as a function of the size (in the same manner as the crossover scale extracted from the peak of the level-spacing distribution). The behavior is very similar to that in the inset in Fig. 3 (although numerical values of the crossover scales differ in the two cases). Both would be consistent with the statement that $J_2^* \to 0$ as $N \to \infty$; however such a conclusion cannot be ascertained on the basis of the data available.
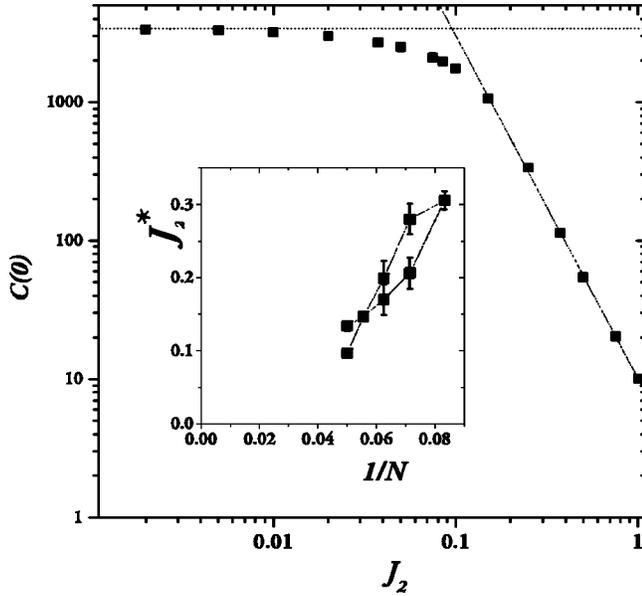
FIG. 7. $C(0)$ as a function of J_2 for $N=20$, $J_1=0.2$, $S^z=3$, $k=0$. The dotted line corresponds to the value at $J_2=0$. The inset shows the finite-size scaling of the crossover scale, $J_2^{*C_0}$, at approximately fixed ratio $S^z/N=1/6$ (for $N=14$, 16, or 20, we pick the two closest values of S^z for these sizes).

V. SPIN STIFFNESS

Now we discuss the effect of the integrability breaking Eq. (5) on the stiffness D_2. In Fig. 2 we show three sets of data corresponding to three different values of the XXZ anisotropy parameter J_1. The data illustrate the following tendencies.

(i) For $0<J_1<1$ (represented by $J_1=0.2$; similar behavior is observed for other values) the data clearly show that very small integrability breaking (characterized by $J_2 =0.01$) has little effect on the stiffness of the finite chains (which is to be expected). Moreover, the extrapolation to infinite size seems to result in a finite value for the stiffness in a manner similar to that of the integrable model.

(ii) For the Heisenberg model, small integrability breaking again does not have a pronounced effect; however, in this case (even though the extrapolation indicates a finite value for the thermodynamic limit), one cannot be certain of the behavior of the infinite chain.

(iii) For $J_1=0$ the situation is different: even a very small amount of integrability breaking leads to a sharp reduction in the stiffness for finite chains. The extrapolation to infinite size is also uncertain. It should be noted, however, that if one compares the behavior of two integrable cases, $J_1=0$ and $J_1>0$, then a similar picture arises (compare, for example, the two top dashed lines in Fig. 2). This has to do with the fact that the spin chain at $J_1=0$ can be mapped (by means of the Jordan-Wigner transformation) onto a system of free spinless Fermions and as such possesses more symmetries than even the integrable (but interacting) XXZ model.

(iv) When the integrability-breaking parameter is not small, the stiffness decays sharply (in fact, if we were to show a log-log plot, faster than any power law) with system size and clearly extrapolates to zero in the thermodynamic limit. This behavior is qualitatively independent of J_1.

Thus the data suggest that for finite chains there exists a "critical" value of J_2 (smaller than the point of the gap opening) beyond which the stiffness tends to vanish. This value is not universal, in the sense that it depends on J_1. This situation is illustrated in Fig. 8, where we show the dependence of the stiffness on J_2 for three values of J_1 and the fixed system size $N=18$. For large values of J_2, all three curves saturate to zero (although the one with $J_1=1$ does so faster). For $J_1=0.2$ the effect of small J_2 is rather weak, and the curve exhibits a clear crossover. For $J_1=0$ the crossover also appears; however, the value 0.08 to which the curve tends as $J_2 \to 0$ is much smaller than the value at $J_2=0$ exactly (which is 0.25 and is thus outside the frame of the plot). The crossover is illustrated in the left inset. The right inset shows the change of the crossover scale with system size for $J_1=0$, 0.2, and 0.4. The behavior at $J_1=1$ is quite different and, in particular, does not show an obvious crossover (and is thus not represented in the right inset). This
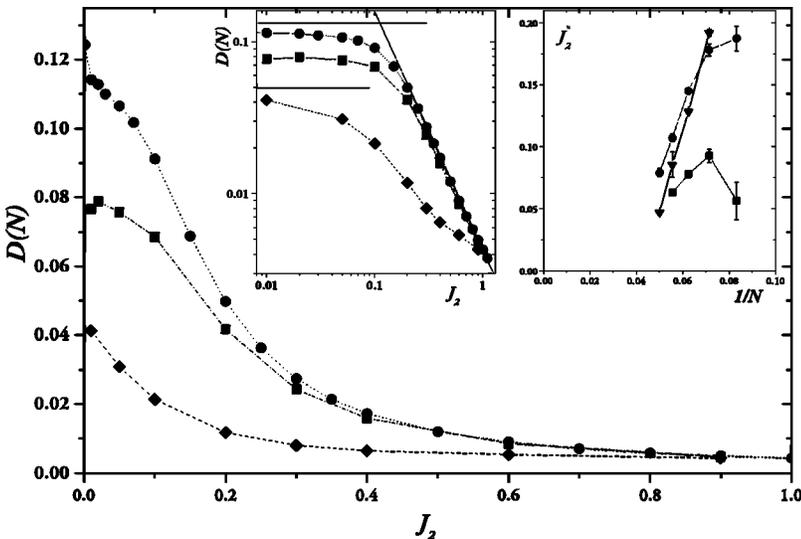

FIG. 8. $D(N)$ as a function of J_2 (for $N=18$). The main plot and the left inset show the same data in linear and log-log scale (meant to illustrate the crossover to a power-law decay of the stiffness at large J_2 for smaller values of J_1) for $J_1=0$ (squares), $J_1=0.2$ (circles), and $J_1=1$ (diamonds). The horizontal lines in the inset indicate the values of $D(N)$ at $J_2=0$ for $J_1=0.2$ (the upper line) and $J_1=1$. The second inset shows the size dependence of the crossover scale for $J_1=0$, 0.2, and 0.4 (triangles). The Heisenberg case $J_1=1$ does not show a clear crossover.

behavior might be related to the conjecture[16] that at the Heisenberg point the stiffness vanishes in the thermodynamic limit even without the integrability breaking. Alternatively, this can reflect the fact that the Heisenberg model is characterized by logarithmic correlations,[15] and thus the small systems considered in this paper are not representative.

VI. DISCUSSION

Prior to performing the calculations one could have had two conflicting expectations for the behavior of the nonintegrable system: (i) as soon as the integrability is broken the system becomes chaotic and as a result shows diffusive transport, (ii) there exists a ''critical'' magnitude of the integrability breaking that separates the chaotic regime from the one that retains some features of the integrable model, in particular, ballistic transport.

The latter picture has an analogy in the localization problem in disordered conductors.[25] The states of an integrable model can be visualized as well-defined localized points in the multidimensional space of the integrals of motion characteristic of the model. These points are well separated due to the quantization of the values of the integrals of motion. Consider now the effect of an infinitesimally small integrability breaking. One can certainly expect the points to spread out into fuzzy spots, but at the same time one might argue that unless the integrability breaking is strong enough, these spots do not overlap. In this regime the system retains some memory of the fact that it was indeed integrable before the extra interaction was turned on. When the integrability breaking is so strong that the spots overlap into a continuum, the system becomes fully chaotic.

The numerical analysis presented in this paper seems roughly consistent with the second possibility for finite chains: a small integrability-breaking term leads to behavior that is close to that of the integrable system. Quantities related to transport, the stiffness D_2 and the ''conductance'' $C(0)$, exhibit a reasonably rapid crossover as functions of the strength of the integrability-breaking interaction. The crossover behaviors seem to be different for different quantities. Table I, for example, illustrates some of this variability for the example of $J_1 = 0.2$, intermediate between the noninteracting model and the Heisenberg point. Similarly, the quantitative characteristics of the level-spacing distribution (namely, the peak position and the tail parameter, see Figs. 3 and 4, or cumulants, see Fig. 5) exhibit similar crossovers

(the corresponding scales are also included in Table I).

The one exception to this picture is the number of degenerate levels in the system[20] represented by $P_\Delta(0)$. This measure exhibits a jump as infinitesimally small (numerically meaning of the order of the computer precision) J_2 is introduced [namely, $P_\Delta(0)$ vanishes, as illustrated in Fig. 1].

One might be tempted to speculate on the universality or otherwise of the crossover from Poisson to Wigner-Dyson statistics. Table I compiles different crossover scales depending on the quantity measured. All the scales appear to decrease with system size, but it is not clear that they do so in the same way: as we have argued, meaningful finite-size scaling of the various J_2^* numbers requires a fixed *filling* rather than fixed S^z. We will note, from the table, that stiffness $D_2 T$ appears the most fragile of the measures, in the sense that it crosses over to the chaotic regime for the smallest integrability-breaking J_2, while the shape of the tail appears the most robust. The tail concerns relatively rare large level spacings, while $D_2 T$ weighs the whole spectrum. Perhaps a small number of ballistic channels could remain open after the latter measure has ceased to count them.

Conclusions for the thermodynamic limit are harder to draw from our data. The variation of crossover scale with system size indicated in the insets to the different figures suggests that the crossover scale vanishes in the limit of an infinite-size system rather than saturating at nonzero values for J_2^*, but the limited range of sizes available to us, along with the absence of a theoretically justified extrapolation to the thermodynamic limit, precludes a definite statement. Constructing a theory of the approach to the infinite-size limit of chains with weak integrability breaking remains an important open problem.

[1] M.L. Mehta, *Random Matrices* (Academic, New York, 1991).

[2] R.J. Baxter, *Exactly Solvable Models in Statistical Mechanics* (Academic, New York, 1982).

[3] C.W.J. Beenakker Rev. Mod. Phys. **69**, 731 (1997); T. Guhr, A. Müller-Groeling, and H.A. Weidenmüller, Phys. Rep. **299**, 189 (1998).

[4] M. Faas, B.D. Simons, X. Zotos, and B.L. Altshuler, Phys. Rev. B **48**, 5439 (1993).

[5] X. Zotos and P. Prelovsek, Phys. Rev. B **53**, 983 (1996).

[6] X. Zotos, F. Naef, and P. Prelovsek, Phys. Rev. B **55**, 11 029 (1997); H. Castella, X. Zotos, and P. Prelovsek, Phys. Rev. Lett. **74**, 972 (1995).

[7] B.N. Narozhny, A.J. Millis, and N. Andrei, Phys. Rev. B **58**, R2921 (1998).

[8] P.H. Song and D.L. Shepelyansky, Phys. Rev. B **61**, 15 546 (2000).

[9] R. Berkovits and Y. Avishai, J. Phys.: Condens. Matter **8**, 389 (1996); see also Y. Avishai, J. Richert, and R. Berkovits, Phys.

Rev. B **66**, 052416 (2002), where a random magnetic field supplies the disorder.

[10] M. DiStasio and X. Zotos, Phys. Rev. Lett. **74**, 2050 (1995).

[11] K. Kudo and T. Deguchi, Phys. Rev. B **68**, 052510 (2003). Our system corresponds to their Eq. (5) with $\alpha = 0$. We cannot agree with their conclusion that in this case, the strength of next-nearest-neighbor coupling [J_2 in our Eq. (5)] "does not change $P(s)$ [the level-spacing distribution] very much." Instead, we characterize how the level-spacing distribution does depend on J_2 and system size.

[12] W. Kohn, Phys. Rev. **133**, A171 (1964).

[13] B.S. Shastry and B. Sutherland, Phys. Rev. Lett. **65**, 243 (1990).

[14] J. des Cloiseaux and M. Gaudin, J. Math. Phys. **7**, 1384 (1966).

[15] P. Ginsparg, in *Champs, Cordes et Phénomènes Critiques =Fields, Strings, and Critical Phenomena*, edited by E. Brézin and J. Zinn-Justin (North-Holland, Amsterdam, 1990).

[16] K. Fabricius and B.M. McCoy, Phys. Rev. B **57**, 8340 (1997). X. Zotos, Phys. Rev. Lett. **82**, 1764 (1999), using a Bethe-Ansatz calculation, confirms this conjecture, but F. Heidrich-Meisner, A. Honecker, D.C. Cabra, and W. Brenig, Phys. Rev. B **68**, 134436 (2003) [among others] find rather a nonvanishing Drude weight. See the latter for a recent bibliography of work addressing this question.

[17] S. Eggert, Phys. Rev. B **54**, R9612 (1996).

[18] The numerical estimates for the opening of the gap are based on the following observation on the XXZ model, where the gap opens (Ref. 14) for $|J_1| > 1$. The ground state of the system in the gapless regime is unique and corresponds to total spin $S^z = 0$. The first excited state is a Heisenberg triplet ($S^z = 1$) and is doubly degenerate away from the Heisenberg point. The next excited state is again a singlet. Now, when the gap opens, the ground state becomes doubly degenerate in the infinite chain, but it is still a singlet. Thus, as one varies slowly the interaction parameter responsible for opening the gap, the nondegenerate excited singlet has to cross the degenerate triplet in order to merge with the ground state. For the XXZ model, this happens as J_1 crosses through the Heisenberg point, at which the three lowest excited states are degenerate. Increasing J_1 should in the thermodynamic limit lead to doubly degenerate ground and first excited states. However, for finite chains this never happens for J_1 slightly exceeding 1. Instead, the spectrum consists of the singlet ground state and the first excited state, with the next excited state being the doubly degenerate triplet. Increasing J_1 reduces the interval between the singlets while increasing the interval between the "excited" singlet and the triplet. For fixed $|J_1| < 1$, the point in J_2 at which one now observes this crossing is a weakly increasing function of system size and of J_1.

[19] In computing levels and the other statistics reported here, we consider only the middle two-thirds of levels, consistent with Ref. 4. This avoids the unrepresentative spacings of extremal eigenvalues in finite systems; qualitative conclusions are independent of the middle fraction (1/3, 2/3, 3/4) employed.

[20] Breaking integrability of course does not break the trivial global conservation laws, such as energy and total spin. In addition Eq. (5) preserves the translational invariance of the XXZ Hamiltonian. Therefore, in order to observe level repulsion one has to restrict oneself to a set of levels with particular values of the total spin S^z and momentum. All the other conservation laws present in the XXZ model are broken by Eq. (5). (Parity also is conserved in the special case $S^z = \phi = 0$; otherwise, we did not find any significant difference between momentum sectors.)

[21] While the choice of the functional forms used to describe the crossovers is somewhat arbitrary, we choose two particular ways to estimate the crossover scales. Parameters of the level-spacing distribution were fitted to a hyperbolic tangent (which illustrates exponential saturation of the peak position and the tail form as the distribution approaches the Wigner-Dyson limit), while the stiffness and level-velocity autocorrelation function were found numerically to exhibit a crossover to a power-law decay for large J_2.

[22] N.G. van Kampen, *Stochastic Processes in Physics and Chemistry* (North-Holland, New York, 1992).

[23] E.S. Keeping, *Introduction to Statistical Inference* (Dover, New York, 1995).

[24] The higher cumulants describe the deviation of a distribution from a Gaussian, for which they are identically zero.

[25] This analogy was suggested by B.L. Altshuler.